Holocene linkages between char, soot, biomass burning and climate from Lake Daihai, China

Y. M. Han,[1] J. R. Marlon,[2] J. J. Cao,[1] Z. D. Jin,[1] and Z. S. An[1]

Received 27 August 2011; revised 23 September 2012; accepted 20 October 2012; published 13 December 2012.

[1] Black or elemental carbon (EC), including soot and char, are byproducts of anthropogenic fossil-fuel and biomass burning, and also of wildfires. EC, and particularly soot, strongly affects atmospheric chemistry and physics and thus radiative forcing; it can also alter regional climate and precipitation. Pre-industrial variations in EC as well as its source areas and controls however, are poorly known. Here we use a lake-sediment EC record from China to reconstruct Holocene variations in soot (combustion emissions formed via gas-to-particle conversion processes) and char (combustion residues from pyrolysis) measured with a thermal/optical method. Comparisons with sedimentary charcoal records (i.e., particles measured microscopically), climate and population data are used to infer variations in biomass burning and its controls. During the Holocene, positive correlations are observed between EC and an independent index of regional biomass burning. Negative correlations are observed between EC and monsoon intensity, and tree cover inferred from arboreal pollen percentages. Abrupt declines in temperature are also linked with widespread declines in fire. Our results 1) confirm the robustness of a relatively new method for reconstructing variations in EC; 2) document variations in regional biomass burning; 3) support a strong climatic control of biomass burning throughout the Holocene; and 4) indicate that char levels are higher today than at any time during the Holocene.

Citation: Han, Y. M., J. R. Marlon, J. J. Cao, Z. D. Jin, and Z. S. An (2012), Holocene linkages between char, soot, biomass burning and climate from Lake Daihai, China, *Global Biogeochem. Cycles*, *26*, GB4017, doi:10.1029/2011GB004197.

1. Introduction

[2] Large increases in atmospheric black carbon (BC) have had substantial impacts on radiative forcing and the hydrologic cycle since industrialization [*Ramanathan et al.*, 2001; *Hansen and Nazarenko*, 2004]. Soot and char are light-absorbing components of BC that can affect climate, but soot is more widely distributed and has a particularly strong effect on areas covered by extensive snow and ice, such as the Arctic and Tibetan glaciers. Soot darkens such surfaces, lowering their albedo and increasing warming [*Ramanathan and Carmichael*, 2008]. Today, black carbon emissions are likely the second strongest contribution to global warming (after carbon dioxide emissions [*Ramanathan and Carmichael*, 2008]). Aerosols including soot have also been shown to have a negative effect on radiative forcing, however, and thus their net effect on climate remains highly uncertain [*Intergovernmental Panel on Climate Change*, 2007]. Pre-industrial BC levels, which originate primarily from vegetation (biomass) burning are estimated to be far smaller than those occurring from today's fossil-fuel burning [*McConnell et al.*, 2007], but BC remains critically important for understanding climate system dynamics because of its large contribution to the land-atmosphere carbon flux [*Patra et al.*, 2005] and to the global methane cycle [*Mischler et al.*, 2009].

[3] Sedimentary charcoal records are the primary source of information about century- to millennial-scale variations in biomass burning [*Whitlock and Larsen*, 2002], and networks of these records have been combined to produce regional and global syntheses [*Carcaillet et al.*, 2002; *Power et al.*, 2008]. There are large uncertainties in paleofire reconstructions however, and large gaps in the network, including in Asia. Also, most charcoal records reflect local burning (within tens of kilometers), which results in high inter-site variability [*Gavin et al.*, 2006]. Ice core records have been used to reconstruct regional and broad-scale changes in biomass burning through analyses of vanillic acid and CO, for example [*McConnell et al.*, 2007; *Wang et al.*, 2010], and further efforts are underway to develop additional fire proxies [e.g., *Eckmeier and Wiesenberg*, 2009] on longer temporal scales, but these approaches are still new and uncertain, and thus far do not span the Holocene. Pre-industrial BC is also produced from biomass burning, but long-term BC records typically span centuries rather than millennia [*Elmquist et al.*,

[1]Key Laboratory of Aerosol Science and Technology, State Key Laboratory of Loess and Quaternary Geology, Institute of Earth Environment, Chinese Academy of Sciences, Xi'an, China.
[2]Department of Geography, University of Wisconsin–Madison, Madison, Wisconsin, USA.

Corresponding author: J. R. Marlon, Department of Geography, University of Wisconsin–Madison, 550 N. Park St., Madison, WI 53706, USA. (marlon@wisc.edu)

0886-6236/12/2011GB004197

2007; *Thevenon et al.*, 2009], and the longest records often have limited sampling resolution records [*Bird and Cali*, 1998; *Thevenon et al.*, 2003]. Importantly, the wide variety of analytical methods for determining BC often produce conflicting results, due not only to measurement error but also to differences in the combustion products identified and the definitions of these products [*Elmquist et al.*, 2006; *Hammes et al.*, 2007; *Conedera et al.*, 2009; *Bird and Ascough*, 2012].

[4] BC is not a single chemical compound or a group with well-defined characteristics, but a suite of compounds occurring along a "combustion continuum" [*Goldberg*, 1985; *Masiello*, 2004]. BC may contain both elemental carbon (EC), which is thermally refractory pure carbon with a graphitic structure, as well as organic carbon (OC) and both efficiently absorb light [*Chow et al.*, 2009]. Two primary types of BC are combustion residues from pyrolysis (char) and combustion emissions formed via gas-to-particle conversion (soot) [*Masiello*, 2004; *Elmquist et al.*, 2006]. Char is produced during pyrolysis by heating organic substances, or as an impure form of graphitic carbon obtained as a residue when carbonaceous material is partially burned or heated with limited access to air. Char is composed mainly of micrometer-sized particles, is less condensed than soot and often retains the morphology of its source material. The countable char particles identified under a microscope (generally >10 μm) are called charcoal. Soot refers only to those carbon particles that form at high temperatures via gas-phase processes. Soot is composed mainly of submicron particles formed by the condensation of hydrocarbon radicals at high temperatures (>600°C). Because soot is more condensed and recalcitrant than char, previous studies have had better success distinguishing soot than char from the broader spectrum of BC compounds [*Elmquist et al.*, 2006].

[5] Char and soot have different chemical and physical properties [*Masiello*, 2004] and thus light-absorbing characteristics [*Bond et al.*, 2002; *Kirchstetter et al.*, 2004; *Andreae and Gelencser*, 2006; *Alexander et al.*, 2008], but there is no absolute or standard measurement technique for them because of their complex characteristics [*Schmidt and Noack*, 2000]. As a result, comparing BC results from different studies has been challenging and artifacts have been reported for each of the different methods currently in use [*Hammes et al.*, 2007]. The primary method for analyzing black carbon in soils and sediments is a chemothermal method (CTO-375), which measures BC in soot form [*Gustafsson et al.*, 1997, 2001]. In aerosol studies, thermal methods are also common [e.g., *Cachier et al.*, 1989; *Fung*, 1990], and more recently, thermal-optical methods [e.g., *Chow et al.*, 1993; *Birch and Cary*, 1996; *Chow et al.*, 2001b; *Cavalli et al.*, 2010]. As just one example of the complications, in the thermal method, some catalysts and ions in samples may decrease the activation energy of BC in the analysis process, leading to negative results (underestimation) [*Novakov et al.*, 2005; *Han et al.*, 2009b]. On the other hand, some water soluble organic carbon (WSOC) not evolved in organic carbon (OC) oxidization steps [*Yu and Ito*, 2002; *Schauer et al.*, 2003] can result in positive results (overestimation). As a result, discrepancies between comparisons of BC measurements using different methods (and potentially different BC or EC definitions) can be more than a factor of 500 [*Schmidt*, 2001; *Hammes et al.*, 2007].

[6] Recently, *Han et al.* [2007b] evaluated the use of thermal optical reflectance (TOR) from the Interagency Monitoring of Protected Visual Environments (IMPROVE), a method commonly used for analyzing carbonaceous aerosols [*Chow et al.*, 2001a; *Gelencsér*, 2004] to differentiate char and soot from EC, which is defined operationally below. The results from this study indicate that pure char material always peaks at the low temperature stage (i.e., EC1, evolving at 550°C in a 2% O2, 98% He atmosphere), whereas pure soot samples peak at the high temperature stage (i.e., EC2 and EC3, evolving at 700°C and 800°C in a 2% O2, 98% He atmosphere, respectively) [*Han et al.*, 2007a]. Comparison of the TOR and chemothermal (CTO-375) methods [*Gustafsson et al.*, 1997, 2001] demonstrate that soot determined by the CTO-375 method corresponds to EC2 and EC3 as found by the TOR method [*Han et al.*, 2007b], suggesting that the TOR method can differentiate between char and soot. This differentiation has since been used in aerosol studies [e.g., *Han et al.*, 2010], as well as in the study of soil and road dusts to assess local air pollution in urban areas [*Han et al.*, 2009a, 2011]. In aerosol studies, the presence of WSOC and certain ions (especially Cl^- and $NO3^-$) can influence the reliability of EC quantification as well as the differentiation between char and soot, however, with sedimentary samples, pretreatment procedures (described below) are employed to remove the WSOC and ions.

[7] Here we employ the TOR method of EC analysis, which has the potential to distinguish between char (EC_{char}) and soot (EC_{soot}) [*Han et al.*, 2007b, 2009b], to reconstruct Holocene variations in EC from Lake Daihai in Inner Mongolia. We compare the EC reconstructions with an independent reconstruction of regional biomass burning based on a composite record of 36 sedimentary charcoal records from eastern Asia [*Marlon et al.*, 2012]. The EC records are also compared with changes in climate, vegetation and human activities to identify potential influences on EC variations.

2. Methods

2.1. Data Collection and Chronology

[8] A 12.08-m long sediment core (DH99-A) was recovered from the center of Lake Daihai (112°40′E, 40°32′N) in 1999 (see auxiliary material Figure S1b in Text S1) using a piston corer driven by a TOHO drilling rig (Model D1-B, Japan).[1] DH99-A contains irregularly laminated, gray-black silt clay. A total of 523 samples from the upper 10.92 m of DH99-A, including a surface sample which was collected in 2001 from the same place, were used for elemental carbon analysis. Multiple chronologies have been developed for the DH99-A and for a second core (DH99-B) from Lake Daihai based on a variety of dates from both cores (Table S1 in Text S1). In total, sixteen ^{210}Pb dates [*Jin et al.*, 2001], twenty-one accelerator mass spectrometry (AMS) radiocarbon dates [*Jin et al.*, 2004; *Xiao et al.*, 2004] and two aragonite U-Th dates analyzed by Thermal Ionization Mass Spectrometry (TIMS) [*Sun et al.*, 2001] are available from both cores (Table S1 in Text S1). In order to maximize the information available from all the available dates, including those that appear too young or old, we used Bayesian age-depth

[1]Auxiliary materials are available in the HTML. doi:10.1029/2011GB004197.

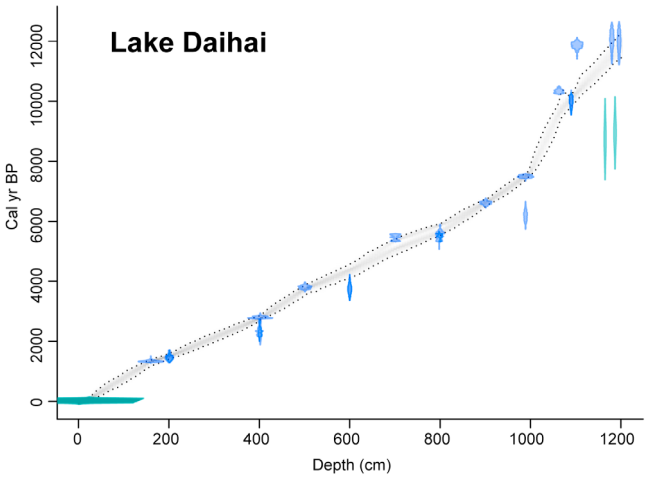

Figure 1. Posterior age–depth model of the sediment cores from Lake Daihai overlaying the calibrated distributions of the individual dates (purple) developed using the Bayesian software "Bacon" [*Blaauw and Christen*, 2011]. Grey dots indicate the model's 95% probability intervals.

modeling software [*Blaauw and Christen*, 2011] to estimate ages and uncertainties for each sample (Table S2 in Text S1). Sediment samples were pretreated with HCl and HF acids to remove carbonates, minerals and metal oxides before carbon analysis using a thermal optical reflectance (TOR) method detailed in *Han et al.* [2007b] and summarized below to differentiate between char and soot [*Han et al.*, 2009b].

2.2. Carbon Analysis

[9] All samples were dried in an oven at 40°C for 2 days. The dried samples were ground in an agate mortar and pestle and passed through a 63-μm sieve. The TOR method was employed for carbon measurement after acid pretreatment [*Han et al.*, 2007b, 2009b] following the IMPROVE protocol. Approximately 0.15 ± 0.05 g of each sample was weighed (1/10,000 balance) and pretreated with HCl and HF acids to remove carbonates, minerals and metal oxides. The residues were filtered onto pre-fired (850°C, 3 h) 47-mm quartz filters for carbon analysis using a DRI Model 2001 Thermal/Optical Carbon Analyzer. Carbon was allowed to evolve through programmed, progressive heating resulting in eight carbon fractions: four organic carbons (OC, comprising OC1, OC2, OC3 and OC4 at 120, 250, 450 and 550°C in pure helium), one pyrolyzed organic carbon (POC, produced in the heating process, and monitored by assessing the return to initial values of laser reflectance) and three EC (EC1, EC2, and EC3 at 550, 700, and 800°C in 2% oxygen and 98% helium). OC is defined as OC1 + OC2 + OC3 + OC4 + POC and EC as EC1 + EC2 + EC3 − POC. EC_{char} is defined as EC1 minus POC and EC_{soot} as the sum of EC2 and EC3 [*Han et al.*, 2007b]. The analyzer was calibrated daily using known quantities of CH_4. Replicate analyses were performed at the rate of one per group of 10 samples. The difference in comparison with the average values from replicate analyses was <10% for EC_{char} and EC_{soot}. In addition to EC, total organic carbon concentrations (TOC) were obtained from *Jin et al.* [2004] who determined the values using a USA CE-440 CHON elemental analyzer after HCl acid pretreatment.

[10] Uncertainty in the estimation of the EC data (Table S2 in Text S1) is calculated as:

$$CV = \frac{\sum_{i=1}^{N} \frac{2 \times |c_i - c_{i,r}|}{c_i + c_{i,r}}}{N}$$

$$Unc_i = \sqrt{(CV \times c_i)^2 + MDL^2}$$

where CV = coefficient of variance; N = number of samples; c_i = concentration of initial analysis; $c_{i,r}$ = concentration of sample "*i*" replicate analysis; Unc_i = uncertainty; *MDL* = minimum detection limit. The replicate analyses in this study are at the rate of one per group of 10 samples, and the reproducibility is better than 8% for EC and better than 10% for ECchar and ECsoot. The average CV for EC, EC_{char} and EC_{soot} from the replicate analyses is used as the common CV for the corresponding carbon content for all samples in this study. The *MDL* of the DRI Model 2001 carbon analyzers is based on the analyses of 214 blank quartz-fiber filters, and is 0.45 μg cm^{-2} for total carbon and organic carbon, and 0.06 μg cm^{-2} for elemental carbon. Here we use 0.06 μg cm^{-2} for EC_{char} and 0.03 μg cm^{-2} for EC_{soot}, respectively, which have been tested in our lab based on the analyses of 20 blank quartz-fiber filters. The MDL in μg cm^{-2} is converted to mass concentrations in mg g-1 based on the weighed amount for each sample. Concentrations were converted to influx values by multiplying by the sedimentation rates calculated from the chronology (Figure 1).

2.3. Comparison of EC Trends With Changes in Climate, Vegetation and Human Activities

[11] An independent published record of regional biomass burning in eastern Asia Multiple was obtained along with data sets on potential factors influencing EC variations for comparison with the EC data, including 1) variations in arboreal pollen percentages from Lake Daihai [*Xiao et al.*, 2004] that indicate a shift from forest to non-forest vegetation, which affected fuel type and flammability; 2) $\delta^{18}O$ data from Greenland [*Stuiver et al.*, 1995] used to infer widespread features of northern hemisphere temperature variations (e.g., a cold interval ca. 8.2 ka); 3) $\delta^{18}O$ data from Dongge [*Dykoski et al.*, 2005; *Wang et al.*, 2005] and Sanbao [*Dong et al.*, 2010] caves used to infer regional monsoon intensity; 4) estimated changes in population and cultivated area (the sum of estimated crop and pastureland) from the HYDE data set [*Klein Goldewijk et al.*, 2010] for 10°–45°N latitude, 65°–150°E longitude; and 5) changes in dynasties in China [*Zhang et al.*, 2008] during the mid- and late- Holocene.

[12] To identify trends in these data and facilitate intercomparisons, the EC data were transformed using a standardization and normalization process described in *Power et al.* [2008] designed to stabilize the variance in the time series and allow statistical analysis. The high-resolution data (i.e., the EC, charcoal, GISP2 and Dongge Cave records) were also smoothed using locally weighted regression (lowess) applied to a 500-year moving window (constant time step) rather than a constant proportion of data (which can vary substantially through time in sediment records) typical of conventional lowess algorithms. For the correlation analyses, transformed but unsmoothed EC data, composite

charcoal data, climate, and pollen data were re-sampled to regular 20-year intervals. Determining the significance of the correlations between the EC, biomass burning and climate proxy data is complicated by temporal autocorrelation in the records that violates an assumption of parametric significance tests. To address this, we used a block-bootstrap method to determine the significance of the correlations [*Gavin et al.*, 2011]. Each bootstrap sample is obtained by resampling (with replacement) the time series in blocks of time corresponding to the autocorrelation structure of the data, determined using the partial autocorrelation function in the R statistical software package [*R Development Core Team*, 2008]. We tested multiple block sizes (from 10 to 30 lags) and report the lowest significance levels found using this range.

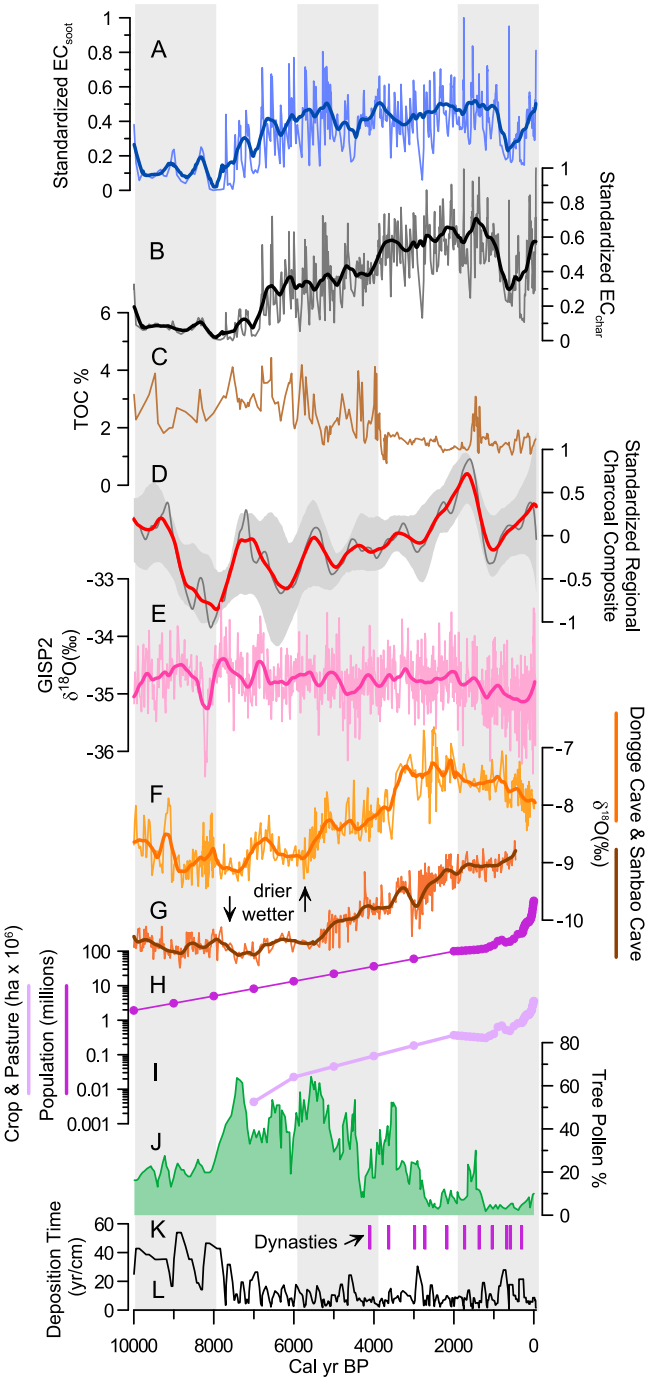

Figure 2. Comparison of (a) standardized EC_{soot} values with (b) standardized EC_{char} values from Lake Daihai; (c) total organic carbon; (d) the composite standardized and smoothed (250- and 500-yr windows) biomass burning record from 36 sites in eastern Asia [*Marlon et al.*, 2012]; (e) GISP2 δ^{18}O data [*Stuiver et al.*, 1995] used to infer northern hemisphere temperature variations; (f) δ^{18}O data from Dongge Cave [*Dykoski et al.*, 2005] and (g) Sanbao Cave [*Dong et al.*, 2010] used to infer regional moisture availability; (h) estimated changes in population and (i) crop and pastureland from the HYDE data set [*Klein Goldewijk et al.*, 2010] for 10°–45°N latitude, 65°–150°E longitude; (j) tree pollen from [*Xiao et al.*, 2004]; (k) changes in dynasties [*Zhang et al.*, 2008]; and (l) deposition times (yr cm^{-1}) based on the age-depth model. High-resolution data (i.e., the EC, Dongge Cave and GISP2 records) were smoothed with a lowess curve using a 500-year moving window.

3. Results and Discussion

3.1. Sampling and Chronology

[13] The chronology used for the EC data are presented in Figure 1. Uncertainties in dating are small for the past 6000 years as the results from *Xiao et al.* [2004] and *Jin et al.* [2004] are generally consistent for the upper 9.0 m. Dating discrepancies occur for the lower 3.08 m, however, with the ages determined by *Xiao et al.* [2004] a little greater than those reported by *Jin et al.* [2004], but those of *Jin et al.* [2004] and *Li et al.* [2004] are similar for this interval (Table S1 in Text S1). Additionally, two aragonite U-Th dates between 11 and 12 m [*Sun et al.*, 2001] analyzed by Thermal Ionization Mass Spectrometry (TIMS) showed much younger ages than those reported by both *Jin et al.* [2004] and *Xiao et al.* [2004]. ^{210}Pb and ^{137}Cs analysis were also previously conducted for the upper part of the DH99-A [*Jin et al.*, 2001], and the sedimentation rates aged by the ^{210}Pb dating, averaging 1.6–1.8 mm a^{-1} are consistent with the youngest AMS ^{14}C dates [*Jin et al.*, 2001].

[14] The Bayesian age-depth analysis yields a nearly linear model for the first 10 m of sediment, with an average Holocene deposition time during of 7.6 yr/cm. The bottom 2 m of sediment, which records early Holocene conditions, show a slower deposition time of about 26.7 yr/cm. While slower sedimentation rates and increased dating uncertainties (observed in both the radiocarbon and U-Th dates) during the earliest period are unfortunate, they are not uncommon in mid- and high-latitude lake sediments. Furthermore, the consistency in estimated ages from *Jin et al.* [2004] and *Li et al.* [2004] from the bottom 2 m of sediment suggests the chronology is robust even in the early Holocene interval, and despite the young estimates from the two aragonite U-Th dates, which may have resulted from detritism.

3.2. Holocene Variations in Soot and Char

[15] Long-term trends in EC_{soot} and EC_{char} showed large variations during the Holocene (Figures 2a and 2b). EC_{soot} fluxes varied from 0.002 to 0.71 mg cm^{-2} yr^{-1} and EC_{char} varied from 0.002 to 2.63 mg cm^{-2} yr^{-1} since 10 ka. In general, mean EC_{soot} and EC_{char} values were low prior to

8 ka and higher after, although a marked decline occurred in the past 2000 years. EC_{soot} levels increased from very low values prior to 8 ka to relatively high values ca. 5 ka. A brief decline in EC_{soot} occurs from 5 - 4 ka, and then levels stabilize until about 1.5 ka. After 1.5 ka, EC_{soot} declines sharply to a local minima ca. 600 and 300 years ago, and then increases rapidly toward present. EC_{char} remains low during the early Holocene prior to 8 ka, and then increases gradually from 8 - 1.5 ka. After 1.5 ka, EC_{char} declines rapidly (like EC_{soot}) to a local minima between ca. 600 and 300 years ago and then increases sharply in the past few centuries.

[16] High-frequency variations in EC_{soot} and EC_{char} also show several shifts during the Holocene. Variability is low, for example, prior to 8 ka, but this is likely due in part to low sedimentation rates (high deposition times) during this period (Figure 2l). High-frequency changes in both EC_{soot} and EC_{char} are relatively consistent from 8 - 2 ka, with the exception of a reduction in variability from about 5 - 4 ka, and an abrupt decline in overall EC values ca. 2.9 ka. Variability in EC_{soot} and EC_{char} appears to increase after 2 ka, and modern EC_{soot} and EC_{char} values in particular are among the highest observed during the Holocene. Holocene EC_{soot} levels surpassed modern values only twice–once ca. 1750 years ago (AD 200) and once ca. 600 years ago (AD 1350) (Figure 2a). The modern EC_{char} value is the highest in the Holocene and surpasses the mean by more than six standard deviations (Figure 2b).

[17] EC_{char} accounts for the largest component of total EC concentrations (86%) and is strongly correlated with total EC ($r = 0.99$; S3 in SI). EC_{soot} is less correlated with total EC ($r = 0.49$; S3 in SI), but EC_{soot} and EC_{char} fluxes are strongly positively correlated ($r = 0.89$). Despite this high correlation, several noticeable differences exist between the standardized EC_{soot} and EC_{char} flux data (Figures 2a and 2b). For example, after 8 ka, EC_{soot} increases immediately, whereas EC_{char} remains relatively low until 7 ka. EC_{char} also shows a steady increase in its mean values from the mid- to late-Holocene (e.g., between 6 and 2 ka), whereas mean EC_{soot} values remain similar during these two periods. EC_{char} also shows a stronger decline between 2 - 1 ka. Thus, although EC_{soot} and EC_{char} appear to reflect a similar underlying process (e.g., biomass burning), differences in EC_{soot} and EC_{char} production, transportation or deposition may account for the observed differences [*Elmquist et al.*, 2006; *Han et al.*, 2010]. A negative correlation between EC_{char} and TOC ($r = -0.64$; $P < 0.001$) and EC_{soot} and TOC ($r = -0.42$; $P < 0.05$) suggests that charring in the analysis has little impact on the EC and EC fractions, and non-pyrogenic matter is not included in the analysis processes using the thermal optical method. EC_{char} and EC_{soot}, which are indicators of biomass burning in this region, are mainly associated with dry conditions (see details of the comparison of EC with the speleothem record below).

3.3. Controls on Holocene Trends in Biomass Burning

[18] Biomass burning is controlled predominantly by climate on regional- to global-scales [*Carmona-Moreno et al.*, 2005]. Seasonal changes in temperature and precipitation, for example, produce a distinct cycle of burning in the northern and southern hemispheres each year [*van der Werf et al.*, 2006]. Vegetation changes also have a strong influence on millennial-scale trends in fire through their effects on fuel characteristics (e.g., abundance, distribution, and flammability). Human activities may have contributed to carbon accumulations in Lake Daihai, but the extent and timing of such human impacts during the Holocene are largely unknown. The charcoal-based biomass burning index as well as data for each of the primary controls on biomass burning–climate, vegetation and human activities–show distinct trends during the Holocene that may help explain the observed changes in EC at Lake Daihai.

[19] The regional biomass burning index (Figure 2d) shows large variations prior to 6 ka, and an upward trend from 6 - 1.6 ka. Biomass burning declines sharply from 1.6 - 1 ka, then rises to AD 1950, and finally declines again to present. Monsoon intensity inferred from the Dongge and Sanbao cave $\delta^{18}O$ values (Figures 2f and 2g) is relatively strong prior to 6 ka, decreases from 6 - 3 ka, and subsequently remains relatively low. There are no regional temperature reconstructions for eastern Asia for the Holocene. The $\delta^{18}O$ data from Greenland indicate a slight and gradual decline in temperatures since about 8 ka at high latitudes, but may have varied from midlatitude temperature trends [*Grafenstein et al.*, 1999]. *Daniau et al.* [2012], for example, suggest that midlatitude temperatures increased during the Holocene and that such changes are consistent with increased biomass burning. Aside from the long-term temperature trends, however, the $\delta^{18}O$ data from Greenland indicate several large short-term changes that are known to be widespread, including a decline in temperatures associated with the "8.2 ka event" [*Alley and Agustsdottir*, 2005] and the Little Ice Age ca. 550 - 250 years ago [*Mann et al.*, 2009].

[20] Vegetation changes near Lake Daihai were reconstructed from changes in the relative abundance of pollen taxa [*Xiao et al.*, 2004] and are representative of broader trends in the region [*Zhao et al.*, 2009]. The primary vegetation types shift from steppe in the early Holocene to steppe forest in the mid-Holocene (8 - 3 ka), to desert steppe in the late Holocene (after ~3 ka). Specifically, arid steppe (high Artemisia, Chenopodiaceae and Ephedra pollen and low arboreal pollen [AP] values) existed from ca. 10 - 8 ka due to a colder-than-present climate and low effective moisture. There is an apparent contradiction between the climate inferred from the vegetation at this time and low $\delta^{18}O$ values in the speleothem records thought to reflect increased monsoon intensity. This discrepancy is widely recognized and may be attributable to low North Atlantic sea-surface temperatures (SSTs) and high-latitude air temperatures that affect the availability, amount and transport of water vapor [*Chen et al.*, 2008]. Between 8 - 3 ka, tree pollen is relatively high and regional climate was generally warmer and wetter than previously. The transition from the mid- to late-Holocene was marked by a shift toward drier conditions, evidenced both by the Dongge Cave $\delta^{18}O$ record and the decline of tree pollen (Figures 2c and 2f). *Xiao et al.* [2004] infer that forest steppe shifted to steppe vegetation during this time due to effectively drier conditions. Today the region is characterized by desert steppe vegetation due to its transitional semi-arid/semi-humid climate.

[21] The population estimates from the HYDE data set show a steady increase during the Holocene (Figure 2h) with the exception of two important events: the Mongol Invasions

Table 1. Statistical Correlations Between EC and Potential Explanatory Variables

EC Data	Potential Explanatory Variable	Correlation
EC_{soot}	Regional charcoal composite	$r = 0.41$; $P < 0.05$
EC_{soot}	Dongge Cave $\delta^{18}O$	$r = 0.66$; $P < 0.001$
EC_{soot}	Arboreal Pollen %	$r = -0.04$; $P > 0.05$
EC_{soot}	GISP2 $\delta^{18}O$	$r = -0.16$; $P > 0.05$
EC_{char}	Regional charcoal composite	$r = 0.51$; $P < 0.01$
EC_{char}	Dongge Cave $\delta^{18}O$	$r = 0.88$; $P < 0.001$
EC_{char}	Arboreal Pollen %	$r = -0.35$; $P < 0.05$
EC_{char}	GISP2 $\delta^{18}O$	$r = -0.23$; $P > 0.05$

starting in AD 1211, when China lost about a third of its population, and the fall of the Ming Dynasty around AD 1644, when it lost about a sixth of its population [*McEvedy and Jones*, 1978; *Pongratz et al.*, 2008]. The land-use area estimates from HYDE show an initial increase beginning 7000 years ago, with variations during the past 2000 years that reflect the changes in population estimates.

[22] Analyses of correlations between the EC data and its potential controls, including the biomass burning and monsoon indexes, as well as temperature proxies and vegetation changes indicate that both EC_{soot} and EC_{char} fluxes have significant positive correlations with biomass burning and negative correlations (although not significantly) with monsoon intensity, TOC content, tree pollen and the Greenland temperature record (Table 1). In particular, EC_{soot} and EC_{char} are both positively correlated with the regional biomass burning index, and the relationship is slightly stronger for EC_{char} ($r = 0.51$, $P < 0.01$) than for EC_{soot} ($r = 0.41$, $P < 0.05$). EC_{char} is also more strongly correlated with the $\delta^{18}O$ values from Dongge Cave ($r = 0.88$, $P < 0.001$) than is EC_{soot} ($r = 0.66$, $P < 0.001$) (higher $\delta^{18}O$ values reflect a weaker monsoon, so there is a negative relationship between biomass burning and monsoon intensity). Finally, EC_{char} (but not EC_{soot}) is negatively correlated with the tree pollen data ($r = -0.35$, $P < 0.05$).

[23] Low EC_{soot} and EC_{char} levels prior to 8 ka imply low biomass burning and are consistent with cool, dry climate conditions (and potentially reduced convection and lightning). Limited vegetation productivity and fuel abundance inferred from the pollen data also likely reduced fire spread (Figure 2j). High charcoal levels from 10 - 9 ka primarily reflect increased burning to the northeast of Lake Daihai [*Li et al.*, 2005], although high burning is common elsewhere in arid steppe environments during the late glacial; this may be partly reflected by moderately high EC values ca. 10 ka (Figures 2a and 2b).

[24] A comparison of EC_{soot} with the GISP2 $\delta^{18}O$ record (Figures 2a and 2e) indicate that both were reduced during the abrupt and widespread cooling that occurred during the 8.2 ka event [*Alley and Agustsdottir*, 2005]. The maximum likely age of the EC samples currently dated to 8 ka is 8.35 ka, and thus it is possible that the minimum in the EC data was synchronous with the 8.2 ka event. Because the independent regional biomass burning record also reaches a minimum ca. 8.2 we argue that the climate changes reduced fire and thus EC_{soot} and EC_{char} levels at 8.2 ka (Figures 2a, 2b, 2d, and 2e). Elsewhere in the world, climate changes often resulted in an opposite effect (i.e., *increased* burning), however [*Marlon et al.*, 2012].

[25] Human activities may be expected to have had an increasing influence on EC_{soot} and EC_{char} trends and/or variability as the Holocene progressed, particularly in the late Holocene with the advent of dynasties in China (Figure 2k) [*Expert Group of the Xia-Shang-Zhou Project*, 2000]. The location of Lake Daihai near the northern limit of intensive agriculture also made it an area of frequent conflict between nomadic tribes and settled farming societies [*Huang and Su*, 2009]. Early Holocene hunter gatherer populations were low, however, EC_{soot} and EC_{char} were low, and charcoal levels were declining, suggesting very limited ecological effects from people on fire prior to 8 ka (Figures 2a, 2b, 2d, and 2h). The earliest large increase in EC_{soot}, EC_{char}, and charcoal occurs between 8 - 7 ka and is associated with a large increase in AP (Figures 2a, 2b, 2d, and 2j), which is also not consistent with widespread human impacts on burning.

[26] Two short-term increases in EC_{char} at 7 ka and 4.1 ka coincide with declines in AP that may reflect localized human impacts on burning through deforestation, but the first *local* evidence for agricultural activity does not occur until 6.3 ka [*Tian*, 2000] and there is no major shift in EC_{soot} or EC_{char} at that time. The second increase in EC_{char} and decline in tree pollen ca 4.1 ka occurs during a period of declining farming and cultural activity following the demise of the Laohushan culture [*Tian*, 2000]. The gradual increase in EC_{char} from 7 - 2 ka parallels a gradual increase in regional human activity (Figures 2h and 2i), but increases in *Pinus* (pine), *Quercus* (oak) and *Ostryopsis* (birch) during the mid-Holocene indicate an expansion of forest steppe vegetation and a shift to generally warm, wet conditions [*Xiao et al.*, 2004] that do not support a strong human impact on burning then. It is possible that fire gradually increased during more frequent but brief intervals of drought during this interval.

[27] A sharp decline in both EC_{soot} and EC_{char} occurs ca. 3 ka coincident with a reduction in regional biomass burning and also with increased effective moisture (Figures 2a, 2b, 2d, and 2g). Subsequently, available moisture declines, AP declines sharply, regional biomass burning increases, and both EC_{soot} and EC_{char} show some of their highest Holocene values; all of this occurs despite a reduction in estimated population growth and land-use (Figures 2a, 2b, 2d, 2f, 2g, 2h, 2i, and 2j). Reduced burning during wet periods and increased fire during dry periods suggests that changes in monsoon intensity or effective moisture continued to exert a strong influence on EC_{soot}, EC_{char} and biomass burning throughout the late Holocene.

[28] The large decline in EC_{soot} and EC_{char} from ca. 2 - 1 ka is matched by a similar decline in biomass burning (Figures 2a, 2b, and 2d) and a final decline in AP (Figure 2j). The lowest late-Holocene EC levels occur around the Little Ice Age (LIA, 550 - 250 years ago [*Mann et al.*, 2009]), but the regional fire decline starts well before the LIA. In central eastern Inner Mongolia [*Huang et al.*, 2005] and the southern loess plateau, burning is thought to be primarily human-caused since 3.1 ka [*Huang et al.*, 2006]. A large fire decline during the past ~600 years in the loess plateau is thought to result from the complete transformation of the landscape to agricultural land and to a lack of vegetation left to burn [*Huang et al.*, 2006], but the HYDE data at least are not consistent with this idea. There is not a unique shift in EC, for example during

the Mongol invasions, and changing dynasties also do not coincide with major EC fluctuations (Figures 2a, 2b, and 2k). Shifts in moisture availability seem a more plausible explanation for the large changes in late-Holocene biomass burning, which are similar across the northern hemisphere [*Marlon et al.*, 2012].

[29] The large variations in biomass burning of the past millennium have implications for debates beyond eastern Asia. The EC minimum 500 years ago in particular parallels a global decline in fire activity at that time, which is roughly coincident with both the onset of the LIA and with the arrival of Europeans in America that led to widespread indigenous population collapse. The fire decline in the tropical Americas is often argued to have reduced global atmospheric CH_4 concentrations from biomass burning [*Ferretti et al.*, 2005; *Houweling et al.*, 2008; *Mischler et al.*, 2009; *Finkelstein and Cowling*, 2011], but whether the decline was triggered by population collapse or reduced temperatures is debated [*Marlon et al.*, 2008; *Nevle and Bird*, 2008; *Dull et al.*, 2010; *Power et al.*, 2012]. The occurrence of a marked regional decline in soot and char in eastern Asia provides important evidence that the fire decline was not limited to the Americas, and thus pandemics associated with European colonization alone cannot account for the decline in Asia. Rather, climate changes or other shifts in human activities must be invoked to explain the widespread fire decline.

[30] In the past 50 years, EC_{soot} and EC_{char} reach very high levels (Figures 2a and 2b). The sources of EC during this interval shift from biomass burning to a combination of biomass and fossil-fuel combustion products, partly reflecting the industrialization of Asia during the latter half of the 20th century. As the Holocene EC records show, similar EC_{soot} levels were only attained about 800 and 2000 years ago, and current EC_{char} levels are higher than at any other time in the Holocene.

3.4. Concluding Discussion

[31] The similarity in char, soot and charcoal trends during the Holocene provide evidence that all three types of data reflect components of biomass burning. The distinction between EC_{soot} and EC_{char} is subtle, but EC_{char} shows consistently higher levels during the late Holocene, and shows a stronger relationship to both climate changes and regional biomass burning. This result strengthens our confidence in the sedimentary EC reconstructions and also suggests that degradation of charcoal, for example, due to differences in production conditions or environmental exposure does not bias the results [*Ascough et al.*, 2011]. In summary, our results 1) confirm the robustness of a relatively new method for reconstructing variations in EC; 2) document variations in regional biomass burning; 3) support a strong climatic control of biomass burning throughout the Holocene; and 4) indicate that char levels are higher today than at any time during the Holocene.

[32] **Acknowledgments.** We thank Patrick Bartlein, Jessica Blois, and Daniel Gavin for software and R scripts used in the data analysis. This study is supported by the National Natural Science Foundation of China (41073102, 40925009 and 41273140), the Knowledge Innovation Program of the Chinese Academy of Sciences (KZCX2-YW-QN113), the National Basic Research Program of China (2010CB833403), the "Strategic Priority Research Program" of the Chinese Academy of Sciences (XDA05100402), and a U.S. National Science Foundation (NSF) Postdoctoral Fellowship to JRM (EAR-0948288).

References

Alexander, D. T. L., P. A. Crozier, and J. R. Anderson (2008), Brown carbon spheres in East Asian outflow and their optical properties, *Science*, *321*, 833–836, doi:10.1126/science.1155296.

Alley, R. B., and A. M. Agustsdottir (2005), The 8 k event: Cause and consequences of a major Holocene abrupt climate change, *Quat. Sci. Rev.*, *24*, 1123–1149, doi:10.1016/j.quascirev.2004.12.004.

Andreae, M. O., and A. Gelencser (2006), Black carbon or brown carbon? The nature of light-absorbing carbonaceous aerosols, *Atmos. Chem. Phys.*, *6*, 3131–3148, doi:10.5194/acp-6-3131-2006.

Ascough, P. L., M. I. Bird, S. M. Francis, B. Thornton, A. J. Midwood, A. C. Scott, and D. Apperley (2011), Variability in oxidative degradation of charcoal: Influence of production conditions and environmental exposure, *Geochim. Cosmochim. Acta*, *75*, 2361–2378, doi:10.1016/j.gca.2011.02.002.

Birch, M. E., and R. A. Cary (1996), Elemental carbon-based method for monitoring occupational exposures to particulate diesel exhaust, *Aerosol Sci. Technol.*, *25*, 221–241, doi:10.1080/02786829608965393.

Bird, M. I., and P. L. Ascough (2012), Isotopes in pyrogenic carbon: A review, *Org. Geochem.*, *42*, 1529–1539, doi:10.1016/j.orggeochem.2010.09.005.

Bird, M. I., and J. A. Cali (1998), A million-year record of fire in sub-Saharan Africa, *Nature*, *394*, 767–769, doi:10.1038/29507.

Blaauw, M., and J. A. Christen (2011), Flexible paleoclimate age-depth models using an autoregressive gamma process, *Bayesian Anal.*, *6*, 457–474, doi:10.1214/ba/1339616472.

Bond, T. C., D. S. Covert, J. C. Kramlich, T. V. Larson, and R. J. Charlson (2002), Primary particle emissions from residential coal burning: Optical properties and size distributions, *J. Geophys. Res.*, *107*(D21), 8347, doi:10.1029/2001JD000571.

Cachier, H., M. Bremond, and P. Buat-Menard (1989), Determination of atmospheric soot carbon with a simple thermal method, *Tellus, Ser. B*, *41*, 379–390, doi:10.1111/j.1600-0889.1989.tb00316.x.

Carcaillet, C., et al. (2002), Holocene biomass burning and global dynamics of the carbon cycle, *Chemosphere*, *49*, 845–863, doi:10.1016/S0045-6535(02)00385-5.

Carmona-Moreno, C., A. Belward, J.-P. Malingreau, A. Hartley, M. Garcia-Alegre, M. Antonovskiy, V. Buchshtaber, and V. Pivovarov (2005), Characterizing interannual variations in global fire calendar using data from Earth observing satellites, *Global Change Biol.*, *11*, 1537, doi:10.1111/j.1365-2486.2005.01003.x.

Cavalli, F., M. Viana, K. E. Yttri, J. Genberg, and J.-P. Putaud (2010), Toward a standardised thermal-optical protocol for measuring atmospheric organic and elemental carbon: The EUSAAR protocol, *Atmos. Meas. Tech.*, *3*, 79–89, doi:10.5194/amt-3-79-2010.

Chen, F., et al. (2008), Holocene moisture evolution in arid central Asia and its out-of-phase relationship with Asian monsoon history, *Quat. Sci. Rev.*, *27*, 351–364, doi:10.1016/j.quascirev.2007.10.017.

Chow, J. C., J. G. Watson, L. C. Pritchett, W. R. Pierson, C. A. Frazier, and R. G. Purcell (1993), The DRI Thermal/Optical Reflectance carbon analysis system: Description, evaluation and applications in U. S. studies, *Atmos. Environ. Part A*, *27*, 1185–1201, doi:10.1016/0960-1686(93)90245-T.

Chow, J. C., J. G. Watson, D. Crow, D. H. Lowenthal, and T. Merrifield (2001a), Comparison of IMPROVE and NIOSH carbon measurements, *Aerosol Sci. Technol.*, *34*, 23–34.

Chow, J. C., J. G. Watson, D. Crow, D. H. Lowenthal, and T. Merrifield (2001b), Comparison of IMPROVE and NIOSH carbon measurements, *Aerosol Sci. Technol.*, *34*, 23–24.

Chow, J. C., J. G. Watson, P. Doraiswamy, L.-W. A. Chen, D. A. Sodeman, D. H. Lowenthal, K. Park, W. P. Arnott, and N. Motallebi (2009), Aerosol light absorption, black carbon, and elemental carbon at the Fresno Supersite, California, *Atmos. Res.*, *93*, 874–887, doi:10.1016/j.atmosres.2009.04.010.

Conedera, M., W. Tinner, C. Neff, M. Meurer, A. F. Dickens, and P. Krebs (2009), Reconstructing past fire regimes: Methods, applications, and relevance to fire management and conservation, *Quat. Sci. Rev.*, *28*, 555–576, doi:10.1016/j.quascirev.2008.11.005.

Daniau, A.-L., et al. (2012), Predictability of biomass burning in response to climate changes, *Global Biogeochem. Cycles*, *26*, GB4007, doi:10.1029/2011GB004249.

Dong, J., et al. (2010), A high-resolution stalagmite record of the Holocene East Asian monsoon from Mt Shennongjia, central China, *Holocene*, *20*, 257–264, doi:10.1177/0959683609350393.

Dull, R. A., R. J. Nevle, W. I. Woods, D. K. Bird, S. Avnery, and W. M. Denevan (2010), The Columbian encounter and the Little Ice Age: Abrupt land use change, fire, and greenhouse forcing, *Ann. Assoc. Am. Geogr.*, *100*, 755–771, doi:10.1080/00045608.2010.502432.

Dykoski, C., R. Edwards, H. Cheng, D. Yuan, Y. Cai, M. Zhang, and Y. Lin (2005), A high-resolution, absolute-dated Holocene and deglacial

Asian monsoon record from Dongge Cave, China, *Earth Planet. Sci. Lett.*, *233*, 71–86, doi:10.1016/j.epsl.2005.01.036.
Eckmeier, E., and G. L. B. Wiesenberg (2009), Short-chain n-alkanes (C16-20) in ancient soil are useful molecular markers for prehistoric biomass burning, *J. Archaeol. Sci.*, *36*, 1590–1596, doi:10.1016/j.jas.2009.03.021.
Elmquist, M., G. Cornelissen, Z. Kukulska, and O. Gustafsson (2006), Distinct oxidative stabilities of char versus soot black carbon: Implications for quantification and environmental recalcitrance, *Global Biogeochem. Cycles*, *20*, GB2009, doi:10.1029/2005GB002629.
Elmquist, M., Z. Zencak, and Ö. Gustafsson (2007), A 700-year sediment record of black carbon and polycyclic aromatic hydrocarbons near the EMEP air monitoring station in Aspvreten, Sweden, *Environ. Sci. Technol.*, *41*, 6926–6932, doi:10.1021/es070546m.
Expert Group of the Xia-Shang-Zhou Project (2000), Results from the Xia-Shang-zhou Projects from 1996 to 2000, *Cultural Relics*, *12*, 49–62.
Ferretti, D. F., et al. (2005), Unexpected changes to the global methane budget over the past 2000 years, *Science*, *309*, 1714–1717, doi:10.1126/science.1115193.
Finkelstein, S. A., and S. A. Cowling (2011), Wetlands, temperature, and atmospheric CO_2 and CH_4 coupling over the past two millennia, *Global Biogeochem. Cycles*, *25*, GB1002, doi:10.1029/2010GB003887.
Fung, K. K. (1990), Particulate carbon speciation by MnO_2 oxidation, *Aerosol Sci. Technol.*, *12*, 122–127, doi:10.1080/02786829008959332.
Gavin, D. G., F. S. Hu, K. Lertzman, and P. Corbett (2006), Weak climatic control of stand-scale fire history during the late Holocene, *Ecology*, *87*, 1722–1732, doi:10.1890/0012-9658(2006)87[1722:WCCOSF]2.0.CO;2.
Gavin, D. G., A. C. G. Henderson, K. S. Westover, S. C. Fritz, I. R. Walker, M. Leng, and F. S. Hu (2011), Abrupt Holocene climate change and potential response to solar forcing in western Canada, *Quat. Sci. Rev.*, *30*, 1243–1255, doi:10.1016/j.quascirev.2011.03.003.
Gelencsér, A. (2004), *Carbonaceous Aerosol*, Springer, Dordrecht, Netherlands.
Goldberg, E. D. (1985), *Black Carbon in the Environment: Properties and Distribution*, John Wiley, New York.
Grafenstein, U. V., H. Erlenkeuser, A. Brauer, J. Jouzel, and S. J. Johnsen (1999), A mid-European decadal isotope-climate record from 15,500 to 5000 years B.P, *Science*, *284*, 1654–1657, doi:10.1126/science.284.5420.1654.
Gustafsson, O., F. Haghseta, C. Chan, J. MacFarlane, and P. M. Gschwend (1997), Quantification of the dilute sedimentary soot phase: Implications for PAH speciation and bioavailability, *Environ. Sci. Technol.*, *31*, 203–209, doi:10.1021/es960317s.
Gustafsson, Ö., T. D. Bucheli, Z. Kukulska, M. Andersson, C. Largeau, J.-N. Rouzaud, C. M. Reddy, and T. I. Eglinton (2001), Evaluation of a protocol for the quantification of black carbon in sediments, *Global Biogeochem. Cycles*, *15*, 881–890, doi:10.1029/2000GB001380.
Hammes, K., et al. (2007), Comparison of quantification methods to measure fire-derived (black/elemental) carbon in soils and sediments using reference materials from soil, water, sediment and the atmosphere, *Global Biogeochem. Cycles*, *21*, GB3016, doi:10.1029/2006GB002914.
Han, Y. M., J. J. Cao, J. C. Chow, J. G. Watson, Z. S. An, Z. D. Jin, K. C. Fung, and S. X. Liu (2007a), Evaluation of the thermal/optical reflectance method for discrimination between char- and soot-EC, *Chemosphere*, *69*, 569–574, doi:10.1016/j.chemosphere.2007.03.024.
Han, Y. M., J. J. Cao, Z. S. An, J. C. Chow, J. G. Watson, Z. Jin, K. Fung, and S. X. Liu (2007b), Evaluation of the thermal/optical reflectance method for quantification of elemental carbon in sediments, *Chemosphere*, *69*, 526–533, doi:10.1016/j.chemosphere.2007.03.035.
Han, Y. M., J. J. Cao, J. C. Chow, J. G. Watson, Z. S. An, and S. X. Liu (2009a), Elemental carbon in urban soils and road dusts in Xi'an, China and its implication for air pollution, *Atmos. Environ.*, *43*, 2464–2470, doi:10.1016/j.atmosenv.2009.01.040.
Han, Y. M., J. J. Cao, E. S. Posmentier, J. C. Chow, J. G. Watson, K. K. Fung, Z. D. Jin, S. X. Liu, and Z. S. An (2009b), The effect of acidification on the determination of elemental carbon, char-, and soot-elemental carbon in soils and sediments, *Chemosphere*, *75*, 92–99, doi:10.1016/j.chemosphere.2008.11.044.
Han, Y. M., J. J. Cao, S. C. Lee, K. F. Ho, and Z. S. An (2010), Different characteristics of char and soot in the atmosphere and their ratio as an indicator for source identification in Xi'an, China, *Atmos. Chem. Phys.*, *10*, 595–607, doi:10.5194/acp-10-595-2010.
Han, Y. M., J. J. Cao, B. Z. Yan, T. C. Kenna, Z. D. Jin, Y. Cheng, J. C. Chow, and Z. S. An (2011), Comparison of elemental carbon in lake sediments measured by three different methods and 150-year pollution history in eastern China, *Environ. Sci. Technol.*, *45*, 5287–5293, doi:10.1021/es103518c.
Hansen, J., and L. Nazarenko (2004), Soot climate forcing via snow and ice albedos, *Proc. Natl. Acad. Sci. U. S. A.*, *101*, 423–428, doi:10.1073/pnas.2237157100.
Houweling, S., G. van der Werf, K. Klein Goldewijk, T. Röckmann, and I. Aben (2008), Early anthropogenic emissions and the variation of CH_4 and $^{13}CH_4$ over the last millennium, *Global Biogeochem. Cycles*, *22*, GB1002, doi:10.1029/2007GB002961.
Huang, C. C., and H. Su (2009), Climate change and Zhou relocations in early Chinese history, *J. Hist. Geogr.*, *35*, 297–310, doi:10.1016/j.jhg.2008.08.006.
Huang, C. C., J. Pang, S. E. Chen, H. Su, J. Han, Y. Cao, W. Zhao, and Z. Tan (2006), Charcoal records of fire history in the Holocene loess-soil sequences over the southern Loess Plateau of China, *Palaeogeogr. Palaeoclimatol. Palaeoecol.*, *239*, 28–44, doi:10.1016/j.palaeo.2006.01.004.
Huang, F., L. Kealhofer, S. Xiong, and F. Huang (2005), Holocene grassland vegetation, climate and human impact in central eastern Inner Mongolia, *Sci. China Ser. D*, *48*, 1025–1039, doi:10.1360/03yd0165.
Intergovernmental Panel on Climate Change (2007), *Climate Change 2007: The Physical Science Basis. Contribution of Working Group I to the Fourth Assessment Report of the Intergovernmental Panel on Climate Change*, edited by S. Solomon et al., Cambridge Univ. Press, Cambridge, U. K.
Jin, Z. D., S. Wang, J. Shen, E. Zhang, F. Li, J. Ji, and X. Lu (2001), Chemical weathering since the Little Ice Age recorded in lake sediments: A high-resolution proxy of past climate, *Earth Surf. Processes Landforms*, *26*, 775–782, doi:10.1002/esp.224.
Jin, Z. D., J. L. Wu, J. J. Cao, S. M. Wang, J. Shen, N. H. Gao, and C. J. Zou (2004), Holocene chemical weathering and climatic oscillations in north China: Evidence from lacustrine sediments, *Boreas*, *33*, 260–266, doi:10.1080/03009480410001280.
Kirchstetter, T. W., T. Novakov, and P. V. Hobbs (2004), Evidence that the spectral dependence of light absorption by aerosols is affected by organic carbon, *J. Geophys. Res.*, *109*, D21208, doi:10.1029/2004JD004999.
Klein Goldewijk, K., A. Beusen, and P. Janssen (2010), Long-term dynamic modeling of global population and built-up area in a spatially explicit way: HYDE 3.1, *Holocene*, *20*, 565–573, doi:10.1177/0959683609356587.
Li, X., J. Zhou, J. Shen, C. Weng, H. Zhao, and Q. Sun (2004), Vegetation history and climatic variations during the last 14 ka BP inferred from a pollen record at Daihai Lake, north-central China, *Rev. Palaeobot. Palynol.*, *132*, 195–205, doi:10.1016/j.revpalbo.2004.06.002.
Li, X., H. Zhao, M. Yan, and S. Wang (2005), Fire variations and relationship among fire and vegetation and climate during Holocene at Sanjiang Plain, northeast China, *Sci. Geogr. Sinica*, *25*(2) 177–182.
Mann, M. E., Z. Zhang, S. Rutherford, R. S. Bradley, M. K. Hughes, D. Shindell, C. Ammann, G. Faluvegi, and F. Ni (2009), Global signatures and dynamical origins of the Little Ice Age and Medieval Climate Anomaly, *Science*, *326*, 1256–1260, doi:10.1126/science.1177303.
Marlon, J., P. Bartlein, C. Carcaillet, D. G. Gavin, S. P. Harrison, P. E. Higuera, F. Joos, M. J. Power, and C. I. Prentice (2008), Climate and human influences on global biomass burning over the past two millennia, *Nat. Geosci.*, *1*, 697–702, doi:10.1038/ngeo313.
Marlon, J. R., P. J. Bartlein, A.-L. Daniau, S. P. Harrison, M. J. Power, W. Tinner, S. Maezumie, and B. Vanniére (2012), Global biomass burning: A synthesis and review of Holocene paleofire records and their controls, *Quat. Sci. Rev.*, in press.
Masiello, C. A. (2004), New directions in black carbon organic geochemistry, *Mar. Chem.*, *92*, 201–213, doi:10.1016/j.marchem.2004.06.043.
McConnell, J. R., R. Edwards, G. L. Kok, M. G. Flanner, C. S. Zender, E. S. Saltzman, J. R. Banta, D. R. Pasteris, M. M. Carter, and J. D. W. Kahl (2007), 20th-century industrial black carbon emissions altered Arctic climate forcing, *Science*, *317*, 1381–1384, doi:10.1126/science.1144856.
McEvedy, C., and R. Jones (1978), *Atlas of World Population History*, Penguin, Harmondsworth, U. K.
Mischler, J. A., T. A. Sowers, R. B. Alley, M. Battle, J. R. McConnell, L. Mitchell, T. Popp, E. Sofen, and M. K. Spencer (2009), Carbon and hydrogen isotopic composition of methane over the last 1000 years, *Global Biogeochem. Cycles*, *23*, GB4024, doi:10.1029/2009GB003460.
Nevle, R. J., and D. K. Bird (2008), Effects of syn-pandemic fire reduction and reforestation in the tropical Americas on atmospheric CO_2 during European conquest, *Palaeogeogr. Palaeoclimatol. Palaeoecol.*, *264*, 25–38, doi:10.1016/j.palaeo.2008.03.008.
Novakov, T., S. Menon, T. W. Kirchstetter, D. Koch, and J. E. Hansen (2005), Aerosol organic carbon to black carbon ratios: Analysis of published data and implications for climate forcing, *J. Geophys. Res.*, *110*, D21205, doi:10.1029/2005JD005977.
Patra, P. K., M. Ishizawa, S. Maksyutov, T. Nakazawa, and G. Inoue (2005), Role of biomass burning and climate anomalies for land-atmosphere carbon fluxes based on inverse modeling of atmospheric CO_2, *Global Biogeochem. Cycles*, *19*, GB3005, doi:10.1029/2004GB002258.
Pongratz, J., C. Reick, T. Raddatz, and M. Claussen (2008), A reconstruction of global agricultural areas and land cover for the last millennium, *Global Biogeochem. Cycles*, *22*, GB3018, doi:10.1029/2007GB003153.

Power, M. J., et al. (2008), Changes in fire regimes since the Last Glacial Maximum: An assessment based on a global synthesis and analysis of charcoal data, *Clim. Dyn.*, *30*, 887–907, doi:10.1007/s00382-007-0334-x.

Power, M., et al. (2012), Sixteenth-century burning decline in the Americas: Population collapse or climate change?, *Holocene*, in press.

Ramanathan, V., and G. Carmichael (2008), Global and regional climate changes due to black carbon, *Nat. Geosci.*, *1*, 221–227, doi:10.1038/ngeo156.

Ramanathan, V., P. J. Crutzen, J. T. Kiehl, and D. Rosenfeld (2001), Aerosols, climate, and the hydrological cycle, *Science*, *294*, 2119–2124, doi:10.1126/science.1064034.

R Development Core Team (2008), *R: A Language and Environment for Statistical Computing*, R Found. for Stat. Comput, Vienna.

Schauer, J. J., et al. (2003), ACE-Asia intercomparison of a thermal-optical method for the determination of particle-phase organic and elemental carbon, *Environ. Sci. Technol.*, *37*, 993–1001, doi:10.1021/es020622f.

Schmidt, M. W. I. (2001), Comparative analysis of black carbon in soils, *Global Biogeochem. Cycles*, *15*, 163–167, doi:10.1029/2000GB001284.

Schmidt, M. W. I., and A. G. Noack (2000), Black carbon in soils and sediments: Analysis, distribution, implications, and current challenges, *Global Biogeochem. Cycles*, *14*, 777–793, doi:10.1029/1999GB001208.

Stuiver, M., P. M. Grootes, and T. F. Braziunas (1995), The GISP2 ^{18}O climate record of the past 16,500 years and the role of the sun, ocean and volcanoes, *Quat. Res.*, *44*, 341–354, doi:10.1006/qres.1995.1079.

Sun, Q. L., J. Zhou, Z. C. Peng, W. G. Liu, and J. L. Xiao (2001), High-precision uranium-series dating of lacustrine carbonates from Daihai Lake, *Chin. Sci. Bull.*, *46*, 588–591, doi:10.1007/BF02900417.

Thevenon, F., E. Bard, D. Williamson, and L. Beaufort (2003), A biomass burning record from the West Equatorial Pacific over the last 360 ky: Methodological, climatic and anthropic implications, *Palaeogeogr. Palaeoclimatol. Palaeoecol.*, *213*, 83–99.

Thevenon, F., F. S. Anselmetti, S. M. Bernasconi, and M. Schwikowski (2009), Mineral dust and elemental black carbon records from an Alpine ice core (Colle Gnifetti glacier) over the last millennium, *J. Geophys. Res.*, *114*, D17102, doi:10.1029/2008JD011490.

Tian, G. J. (2000), The relationships between archaeological culture and ecological environment, Daihai Lake area, in *Research in Environmental Archaeology*, edited by K. S. Zhou and Y. Q. Song, pp. 72–80, Science Press, Beijing.

van der Werf, G. R., J. T. Randerson, L. Giglio, G. J. Collatz, and P. S. Kasibhatla (2006), Interannual variability in global biomass burning emission from 1997 to 2004, *Atmos. Chem. Phys.*, *6*, 3423–3441, doi:10.5194/acp-6-3423-2006.

Wang, Y., H. Cheng, R. L. Edwards, Y. He, X. Kong, Z. An, J. Wu, M. J. Kelly, C. A. Dykoski, and X. Li (2005), The Holocene Asian Monsoon: Links to solar changes and North Atlantic climate, *Science*, *308*, 854–857, doi:10.1126/science.1106296.

Wang, Z., J. Chappellaz, K. Park, and J. E. Mak (2010), Large variations in southern hemisphere biomass burning during the last 650 years, *Science*, *330*, 1663–1666, doi:10.1126/science.1197257.

Whitlock, C., and C. P. S. Larsen (2002), Charcoal as a fire proxy, in *Tracking Environmental Change Using Lake Sediments*, edited by J. P. Smol, H. J. B. Birks, and W. M. Last, pp. 75–97, Kluwer Acad., Dordrecht, Netherlands, doi:10.1007/0-306-47668-1_5.

Xiao, J., Q. Xu, T. Nakamura, X. Yang, W. Liang, and Y. Inouchi (2004), Holocene vegetation variation in the Daihai Lake region of north-central China: A direct indication of the Asian monsoon climatic history, *Quat. Sci. Rev.*, *23*, 1669–1679, doi:10.1016/j.quascirev.2004.01.005.

Yu, Z., and E. Ito (2002), A 2100-year trace-element and stable-isotope record at decadal resolution from Rice Lake in the northern Great Plains, USA, *Holocene*, *12*, 605–617, doi:10.1191/0959683602hl571rp.

Zhang, P., et al. (2008), A test of climate, sun, and culture relationships from an 1810-year Chinese cave record, *Science*, *322*, 940–942, doi:10.1126/science.1163965.

Zhao, Y., Y. Zicheng, and C. Fahu (2009), Spatial and temporal patterns of Holocene vegetation and climate changes in arid and semi-arid China, *Quat. Int.*, *194*, 6–18, doi:10.1016/j.quaint.2007.12.002.